

ARTICLES

Mechanism of Strong Luminescence Photoactivation of Citrate-Stabilized Water-Soluble Nanoparticles with CdSe Cores

Ying Wang,^{†,‡} Zhiyong Tang,[†] Miguel A. Correa-Duarte,^{||} Isabel Pastoriza-Santos,^{||} Michael Giersig,[⊥] Nicholas A. Kotov,^{*,†,‡,§} and Luis M. Liz-Marzán^{*,||}

Department of Chemical Engineering, Department of Materials Science and Engineering, and Department of Biochemical Engineering, University of Michigan, Ann Arbor, Michigan 48109, Departamento de Química Física, Universidade de Vigo, 36310 Vigo, Spain, and Center of Advanced European Studies and Research (CAESAR), Ludwig-Erhard-Allee 2, 53175 Bonn, Germany

Received: March 9, 2004; In Final Form: July 26, 2004

CdSe and CdSe@CdS semiconductor nanocrystals have been synthesized in aqueous solutions, using sodium citrate as a stabilizer. Although initially these quantum dots display photoluminescence with very low quantum yields, upon prolonged illumination with visible light, enhancements up to 5000% have been measured. This leads to aqueous quantum dots with high luminescence, which can have important implications in biological and other applications. A distinct correlation between the photocorrosion process and the photoactivation process is observed. The primary reason for luminescence enhancement is considered to be the smoothing of the CdSe core surface. Importantly, even stronger activation was observed in silica- and CdS-coated nanocolloids where the CdSe core was expected to be shielded from photocorrosion. Preferential adsorption of oxygen molecules in the porous silicate shell accelerates the photocorrosion process. In CdS-coated particles, incomplete coating of the original particles is postulated, which is accompanied by the reforming of the CdS coat because of ionic diffusion at the interface on the newly opening areas with smoother surfaces.

Introduction

Nanocrystals of II–VI semiconductors have generated tremendous interest over the past decade and are often considered for different applications, ranging from light-emitting diodes to biological sensors.^{1–7} This interest arises from the possibility of tuning the optical properties of semiconductor nanocrystals by simply varying their size, owing to the effect of quantum confinement.^{8–10} Among various kinds of materials, colloidal CdSe quantum dots are undoubtedly the most widely studied because of their tunable emission in the visible range and the advances in their preparation.

In semiconductor quantum dots, high emission efficiency from band-edge states is required for both the theoretical study of their electronic structures and any practical applications. Unfortunately, low luminescence quantum yield (QY) is often observed in as-prepared nanoparticles (NPs). Because of their high surface area, nonradiative recombination at surface sites and surface traps compete with band-edge emission.¹¹ This is particularly characteristic of synthetic processes in aqueous

media, although the aqueous methods would be otherwise preferred because of simplicity and environmental concerns. The optimization of NP synthesis conditions has greatly improved the luminescence quantum efficiency. The synthesis of CdSe NPs in trioctylphosphine oxide (TOPO) at high temperature has become one of the most mature and popular ways to achieve high-quality nanocrystals in which the number of surface defects is lower than in other preparations.^{12–14} In this method, reaction temperatures above 250 °C are needed to anneal the surface crystal structure. However, the resulting NPs are soluble only in low polarity solvents such as toluene and chloroform. Further surface modification is necessary to obtain water-soluble materials, which are most often used in biological applications.^{5,6} Another way to increase the QY of nanocrystals is to add a small amount of a second component during the synthesis. For instance, doped NPs such as ZnS/Mn²⁺ show an increase in the luminescence quantum-efficiency scaling with dopant concentration in the nanocrystals,¹⁵ but this way is applicable only to a limited number of nanomaterials. Additionally, simple, reproducible, and environment-friendly methods are highly desirable for semiconductor NP synthesis.

Other strategies to enhance the QY aim to reduce nonradiative recombination by confining the wave function of electron–hole pairs to the interior of the crystals. This is achieved by either passivation with long-chain organic surfactants or epitaxially growing an inorganic shell of material with a larger band gap around each particle. The latter strategies have been shown to

* Corresponding authors. (N.A.K.) E-mail: kotov@umich.edu. Fax: +1-734-764-7453. (L.M.L.-M.) E-mail: lmarzan@uvigo.es. Fax: +34-986-812556.

[†] Department of Chemical Engineering, University of Michigan.

[‡] Department of Materials Science and Engineering, University of Michigan.

[§] Department of Biochemical Engineering, University of Michigan.

^{||} Universidade de Vigo.

[⊥] Center of Advanced European Studies and Research.

improve dramatically the luminescence quantum yield of II–VI semiconductor nanomaterials such as CdS@Cd(OH)₂,¹⁶ CdSe@ZnSe,^{17,18} CdSe@ZnS,^{19,20} CdS@HgS@CdS,^{21,22} and CdSe@CdS.^{23,24}

Photoactivation of the NPs luminescence, that is, an order of magnitude or more increase of QY, is a new process of preparation of highly luminescent nanocolloids. It can be considered to be an important alternative way to achieve high QY. In addition to that photoactivation opens a possibility for new photolithographic processes and the production of patterned surfaces without alterations in the topography of the surface, which are common for other techniques.²⁵ Also, the light-induced transition from the dark state to the bright luminescence state can be the foundation for new technologies in cell tagging and cryptography.²⁶

Several examples of photoactivation were discussed over the past few years. Bol et al.²⁷ observed an increase in QY after doped ZnS/Mn NPs were irradiated by UV light. They also found that prolonged UV irradiation (hours to days) in the presence of water and oxygen led to color change and a decrease in the luminescence quantum efficiency. A laser-induced increase in the photoluminescence QY of CdSe@CdS or CdSe@ZnS core–shell nanodots has also been achieved.²⁸ However, the experimental results indicated that the same laser treatment on CdSe nanorods did not significantly increase their QY, which remained constant or even decreased during irradiation. The photoactivated luminescence of CdSe quantum-dot monolayers has been reported.²⁹ Light-induced alterations in the surface states following the adsorption of water results in quasi-reversible luminescence changes in the quantum dots. In these examples, TOP/TOPO–CdSe NPs were employed. More recently, Jones et al.³⁰ reported the enhancement of CdSe and CdSe@ZnS quantum dots that were stabilized with TOPO in organic solvents upon illumination above the band gap and concluded that this was due to light-activated stabilization of surface traps. The QY for these preparations increased from 0.3 to 13.8%. We note that the actual mechanism of the photoactivation process is not necessarily the same for all of these systems.

In this report, we demonstrate that a simple method for the synthesis of water-soluble CdSe and CdSe@CdS nanocrystals can yield high-luminescence QY colloids upon illumination. The formation of citrate-stabilized CdSe core NPs is induced by microwave irradiation, with reaction times below 1 minute. The citrate ions provide the nanoparticles with sufficient electrostatic stabilization to avoid agglomeration for long periods of time. When the as-prepared NPs (with and without different shells) are exposed to ambient light for an extended period of time, their QY increases dramatically.²⁵ For the core–shell NPs, usually 20–50 times higher photoluminescence emission can be obtained. The maximum quantum yield measured for our core–shell NPs reaches 59.0%. Apart from thiol-stabilized Te-based nanocolloids,^{31,32} the obtained luminescence efficiency is probably the highest among reported data for aqueous CdSe dispersions. Although the size distribution needs to be improved in these dispersions, the QY in them is comparable to the upper limit of the reported quantum yield for semiconductor NPs from organic solvent syntheses. Qualitative and quantitative arguments are presented about the mechanism of the photoactivation process. It is clearly related to the photooxidation of the surfaces of nanocolloids, which is well known to occur in chalcogenide NPs in water when oxygen is present³³ but was not expected to result in such a strong enhancement of luminescence. Such high photosensitivity is unique to the CdSe made as described here

and provides this system with a great potential in applications not only in micropatterning²⁵ but also in data storage materials and sensors.

Experimental Section

Citrate-stabilized CdSe nanocrystals were prepared according to a previously published procedure.²⁴ To 45 mL of water were added 0.05 g of sodium citrate (Aldrich) and 2 mL of 4×10^{-2} M cadmium perchlorate (Aldrich), and the pH was adjusted to 9.0 with 0.1 M NaOH. After the solution had been bubbled with nitrogen for 10 min, 2 mL of 1×10^{-2} M *N,N*-dimethylselenourea (Aldrich) was added, and the mixture was heated in a conventional 900-W (Sharp) microwave oven for 50 s. By varying the CdClO₄ concentration, it was possible to synthesize CdSe nanocrystals with various sizes. For the preparation of core–shell CdSe@CdS nanocrystals to a given volume of CdSe NPs solution as prepared, we added a solution of thioacetamide (4×10^{-2} M, Aldrich) in a quantity such that the molar ratio of $S_{\text{added}}/Se_{\text{initial}}$ was 1:1. The mixture was then heated in a sealed round-bottom flask inside a silicon oil bath to 70–80 °C for 24 h.

Silica coating was carried out by a method previously reported for coating CdS.³⁴ Briefly, to 50 mL of the NP colloid were added, in turn, 0.050 mL of 1 mM mercaptopropyltrimethoxysilane (MPS, Aldrich) and 2 mL of 0.54 wt % sodium silicate solution (pH 10–11) under vigorous magnetic stirring. The resulting dispersion (pH 8.5) was then allowed to stand for 5 days, resulting in the deposition of 6–8-nm-thick silica shells.

The photoactivation of NPs was carried out either in the ambient atmosphere or inside a glovebox under nitrogen. The colloid solution contained in a glass bottle was exposed to ambient light without any other special light source.

UV–vis absorption spectra were taken with a HP8453 diode array Agilent spectrophotometer. Photoluminescence spectra were measured on a modular Fluorolog 3 SPEX spectrofluorometer. Photoluminescence quantum efficiencies of NPs in water were calculated by comparing their integrated emission to that of a solution of rhodamine B in ethylene glycol. Optical densities of all solutions were adjusted to values between 0.1 and 0.25 at the excitation wavelength to avoid reabsorption effects.

The zeta potentials were measured with a Malvern Zetasizer 2000 using the electrophoretic mobility technique.

Scanning tunneling spectroscopy measurements were performed in air by using a Nanoscope IIIa system (Digital Instruments Inc., Santa Barbara, CA) operating in the tapping mode.

High-resolution transmission electron microscopy (HRTEM) was performed in a Philips CM12 microscope operating at 120 kV that was equipped with a high-resolution lens and a 9800 EDAX analyzer. Samples were prepared by letting a drop evaporate on top of a carbon-coated copper grid.

Results

Preparation of Nanocrystals. The absorption spectra of solutions of both naked CdSe and CdSe@CdS core–shell NPs show a peak corresponding to the first excitonic transition (Figure 1). Particle sizes can be controlled through changes in the mole ratio of Cd to Se in the precursor solutions, providing a tunability of the excitonic emission in the visible region, albeit to a lesser extent than for TOPO-capped CdSe nanocrystals. After coating the CdSe NPs with a CdS shell, both absorption and luminescence bands undergo a shift toward lower energies, due to some expansion of the volume available for the exciton

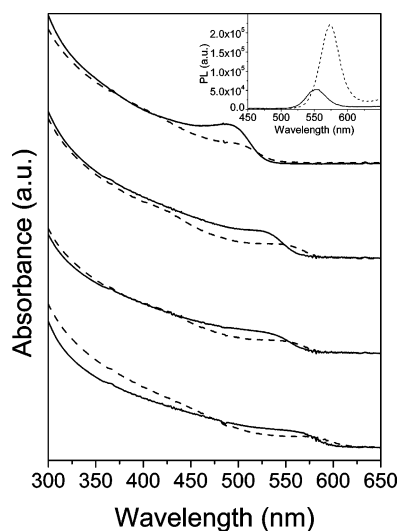


Figure 1. Absorption spectra of various naked CdSe (—) and CdSe@CdS core-shell NPs (---), with average core sizes ranging from 1 to 5 nm (top to bottom) corresponding to Cd/Se ratios of 16:1, 10:1, 8:1, and 4:1. (Inset): Photoluminescence spectra of CdSe (—) and CdSe@CdS (---) nanocrystals with a Cd/Se ratio of 10:1.

generated in the CdSe core, into the CdS shell. The absorption edge red shifts 3–4 nm for all particle sizes, as shown in Figure 1, whereas the luminescence maximum correspondingly red shifts 5–10 nm (inset of Figure 1). Because of the partial overlap of the emission peaks of NPs with different sizes, the inset of Figure 1 shows only photoluminescence spectra of CdSe core and CdSe@CdS core-shell nanocrystals with a Cd/Se ratio of 10:1. In comparison with that of rhodamine B, the room-temperature excitonic emission of CdSe NPs is weak, ca. 0.01–0.40%. Upon deposition of a CdS shell over the CdSe cores, the luminescence intensity increases by 5–10 times. However, the freshly synthesized core-shell NPs still show a luminescence efficiency that is typically below 3.0%. Concerning the mechanism of luminescence enhancement through the deposition of an inorganic shell over the CdSe QDs, it is well known that such a shell passivates NP surface defects, thus leading to the localization of photoexcited charge carriers in the CdSe core.^{9,19} Correspondingly, the nonradiative emission is reduced, whereas the band-edge emission is enhanced.

Photoactivation of CdSe and CdSe@CdS Nanocolloids in Air. Both freshly made CdSe and CdSe@CdS nanocrystals show very weak luminescence. The reasons for such a low quantum yield can be numerous: defects in the crystal lattice, surface structures, and particle clustering. Regardless of the multiple contributions in the nonradiative transitions, it was found that light-irradiated samples showed a significant increase in quantum efficiency, possibly affecting all of the above-mentioned properties simultaneously. To gain further insight into the influence of visible light on luminescence enhancement, QYs were measured at various illumination times.

Figure 2 shows several absorption and emission spectra after different irradiation times for CdSe@CdS NPs (Cd/Se 8:1). The optical densities of all of the samples noticeably decreased during the illumination (Figure 2A). The corresponding band-gap emission peak grew dramatically, at least 2 orders of magnitude in peak intensity, retaining about the same peak width of 35–50 nm. The quantum yield increased from 0.2% for the unexposed sample up to 41.4% for the sample irradiated for 15 days. It can also be observed that light treatment promoted spectral shifts toward shorter wavelengths both in absorption and luminescence, which is consistent with a possible decrease

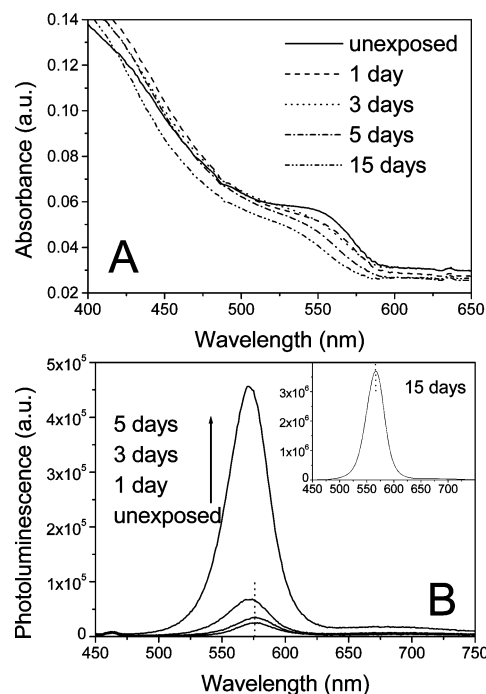


Figure 2. Absorption (A) and emission (B) spectra of CdSe@CdS nanocrystals (Cd/Se 8:1) measured after different irradiation times in air. (Inset in B): Luminescence spectrum after exposure to light for 15 days. Because of the drastic difference in luminescence intensity compared with that of the unexposed sample, this profile is illustrated separately.

of particle size during illumination. For this particular sample, the PL peak blue shifted by 14 nm after illumination for 15 days, which indicates the decrease in particle size.

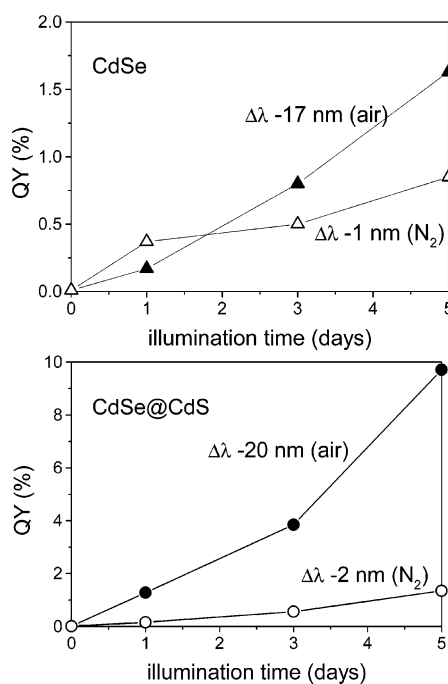
A remarkable increase in luminescence was observed for all core-shell samples upon photoactivation, whereas solutions of unexposed NPs stored in the dark for similar periods of time maintained low QYs. QY and wavelength shifts (minus signs indicate blue shifts) for various NP sizes and illumination times are summarized in Table 1. The QY increase varies with particle size: the smaller particles, with a larger Cd/Se mole ratio, show higher luminescence yields (Table 1), as expected from the basics of quantum confinement effects.³⁵ The accompanying blue shift is, however, more pronounced in larger dots, which is illustrated by a larger $\Delta\lambda$ of -21 nm, for CdSe@CdS with a Cd/Se ratio of 4:1, whereas for the smaller particles (Cd/Se 16:1), the emission peak shifts by only -11 nm. For all of the systems studied, the highest QY measured was as high as $59 \pm 3.5\%$.

In similar experiments, the influence of photoactivation on bare CdSe NPs was also investigated. In general, the QY of photoactivated CdSe NPs was 20–100 times higher than the initial “dark” value. Comparing with that of core-shell NPs of the same core diameter, the luminescence of the uncapped nanocrystals was 2–8 times lower, which was expected from the passivation of the surface traps observed in TOP/TOPO-stabilized systems.^{19,20} More pronounced fluorescence peak shifts were observed during the photoactivation of bare CdSe NPs. For CdSe with a Cd/Se mole ratio of 4:1, the emission peak blue shifted with $\Delta\lambda = -30$ nm, whereas for smaller particles, blue shifts with $\Delta\lambda = -14$ nm were observed. Gradual low-energy shifts of CdSe quantum-dots spectra illuminated in air have been previously observed in room-temperature luminescence from single quantum dots and were attributed to photooxidation of the surface.³⁶

TABLE 1: Quantum Yield and Blue Shift of the Maximum in Emission Spectra during Photoactivation of CdSe and CdSe@CdS Nanoparticles in Air

sample	Cd/Se mole ratio	quantum yield (%)				maximum ^b	$\Delta\lambda$ (5D ^a) nm	$\Delta\lambda$ (15D ^a) nm
		unexposed	3D ^a	5D ^a	15D ^a			
CdSe	4:1	0.01	0.8	1.6	2.0	16(\pm 2.5)	-17	-30
CdSe	8:1	0.2	3.0	7.9	13.6	20(\pm 0.5)	-19	-24
CdSe	16:1	0.3	3.2	6.9	7.2	^c	-7	-14
CdSe@CdS	4:1	0.1	3.9	9.7	17.0	51(\pm 4.0)	-20	-21
CdSe@CdS	8:1	0.2	0.7	6.2	41.4	59(\pm 3.5)	-10	-14
CdSe@CdS	16:1	2.1	12.8	13.4	23.7	^c	-8	-11

^a The notations 3D, 5D, and 15D refer to the number of days the samples were exposed to ambient light. ^b The data in this column are the maximum observed quantum yields during photoactivation. For bare CdSe NPs, the highest QY is usually observed after exposing the sample to light for 30 days, and for CdSe@CdS core-shell NPs, QY shows peak value 25–30 days after photoactivation. ^c Upon increasing the Cd/Se ratio, the NPs are not stable and precipitate quite soon compared to other NPs with a lower Cd/Se ratio. Because the precipitate is still highly luminescent, we prefer to be conservative, giving the exact values of QYs for comparison with other techniques.

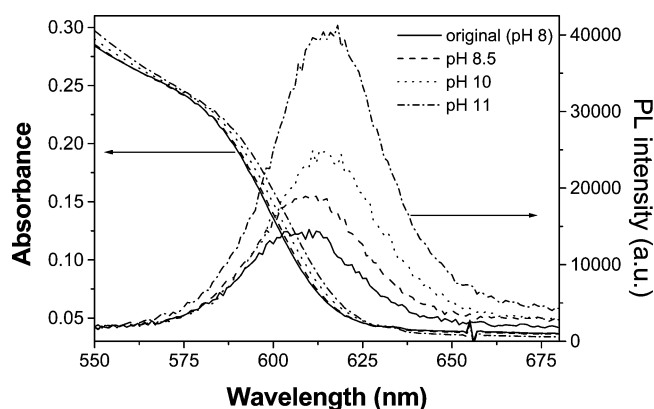
**Figure 3.** Effect of the atmosphere on the QY enhancement during photoactivation. CdSe (Δ , \blacktriangle) and CdSe@CdS (\circ , \bullet) NPs (Cd/Se ratio 4:1) were exposed to light in air (\blacktriangle , \bullet) and in nitrogen (Δ , \circ).

Neither photoactivated bare nor core-shell NPs stored in the dark showed a large QY enhancement, whereas the QY keeps growing upon exposure to ambient light. Usually, the NPs reach their maximum luminescence efficiencies within 1 month. Thereafter, precipitation is observed, but unexpectedly, the precipitate still shows a high luminescence.

Influence of Oxygen on Luminescence Enhancement.

Because oxygen has been demonstrated to play a major role in photooxidation,³³ we decided to investigate the influence of air on the photoinduced luminescence enhancement. After the sample container was flushed with nitrogen, to ensure an oxygen-free environment during the experiment, both CdSe and CdSe@CdS colloids were irradiated while stored under nitrogen in a glovebox.

The time evolution of the quantum efficiencies for CdSe and CdSe@CdS NPs during light irradiation in air and in nitrogen is exemplified in Figure 3. It is clear that the photoluminescence enhancement in nitrogen was far less pronounced than that in air. Although for CdSe NPs the QY remained below 2.0% after 5 days of irradiation (for this particular sample) both in air and in N₂, the difference is more obvious for core-shell NPs, which reached 9.8% when irradiated in air but only 1.3% when

**Figure 4.** Absorption and photoluminescence spectra of freshly made CdSe@CdS (Cd/Se 2:1) colloids at different pH values, as indicated. The sample at pH 8 is the original solution before pH adjustment.

irradiated in N₂. In fact, some enhancement of luminescence for illumination in nitrogen is attributed to the presence of residual amounts of oxygen in the glovebox. Contrary to what was observed during irradiation in air, there was only random spectral diffusion in time, and basically no shift was observed for samples kept under N₂. Similar results were reported for single CdSe@ZnS core-shell quantum dots that were synthesized in TOP/TOPO, which were investigated by spectrally and temporally resolved confocal microscopy, observing a large, $\Delta\lambda = -30$ nm blue shift in the emission wavelength during illumination in air but no blue shift under nitrogen.³⁷ During photoactivation in the inert atmosphere, we found that prolonged irradiation for more than 10 days caused abundant precipitation and luminescence quenching. Thus, we were unable to obtain information about photoactivation over longer periods of time. From the experiments described above, it is obvious that air plays a critical role in the photoactivation process.

Influence of pH on Luminescence Enhancement. An additional piece of information was obtained by studying the effect of the pH of the solution prior to illumination on the photoactivation of the NPs (both CdSe and CdSe@CdS), and the results are shown in Figure 4. The solution pH was adjusted to basic values using 0.5 mM NaOH solution, and PL spectra were measured using the same conditions. The PL intensity increased ca. 3 times when the pH was varied from 8 to 11 without any illumination.

Although there is a noticeable difference in luminescence intensity in the starting samples depending on pH, the emission after enhancement is basically identical, regardless of pH, when illumination is performed in air (after a gradual increase with time; see Figure 5). This indicates that (1) surface processes

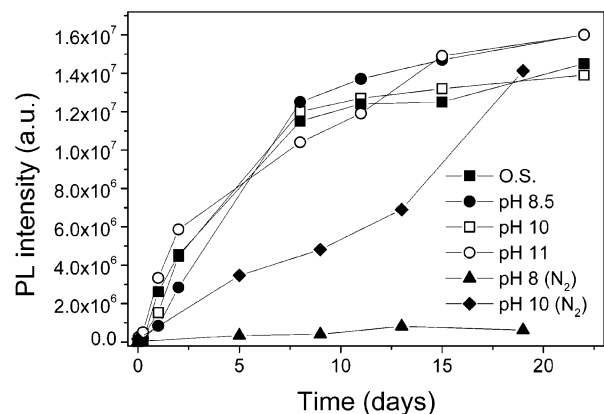


Figure 5. Time evolution of the photoluminescence intensity of CdSe@CdS dispersions adjusted to different pH values in air and under nitrogen. Sample at pH 8 is the original solution before pH adjustment.

TABLE 2: Variation of Zeta Potential upon Irradiation of NP Solution

sample	zeta potential	
	unexposed (mV)	exposed for 5 days (mV)
CdSe@CdS	-42.3	-21.3
CdSe	-48.4	-39.4

play the key role in the photoenhancement phenomenon and (2) the final surface structure of the NPs in the highly luminescent state is characterized by smaller chemical variability, hence a weaker dependence on environmental factors. However, there is a drastic difference when samples are illuminated under the inert atmosphere. Although the original sample basically shows no enhancement in nitrogen at pH 8, the sample previously adjusted to pH 10 shows a clear enhancement, which is initially slower than that for samples in air. As expected, the band shift is much lower for illumination under nitrogen (4 nm after 16 days) than in air (17 nm after 15 days) because photocorrosion does not take place in the inert atmosphere.³⁸

Light-Induced Change of Surface Charges. To elucidate the mechanism of photoactivation, the variation of the surface charge during the process was investigated. The surface charges were determined through electrophoretic mobility measurements, from which zeta-potential values were obtained. Table 2 shows the variation of the zeta potential upon irradiation of NPs in air.

As expected, both the CdSe and CdSe@CdS NPs have negative charges, arising from the presence of citrate ions on their surface. From Table 2, it is clear that the surface charge consistently decreased after the photoactivation process had taken place.

Scanning Tunneling Spectroscopy. To confirm that the drop in surface charge was not caused by solvent effects, we performed scanning tunneling spectroscopy (STS) measurements on single nanocrystals. For STS, highly oriented pyrolytic graphite (HOPG) was used as the substrate for scanning. One drop of unexposed CdSe or CdSe@CdS NPs was spread on the freshly cleaved HOPG surface. After the first scan of the nonphotoactivated sample, the slide was exposed to light for 5 days, and STS measurements were carried out on the same slide. We note that photoactivation occurs not only in solution but also in solid samples, as previously demonstrated on layer-by-layer assembled films.²⁵ Examples of the STS curves obtained for CdSe@CdS with a Cd/Se ratio of 4:1 are shown in Figure

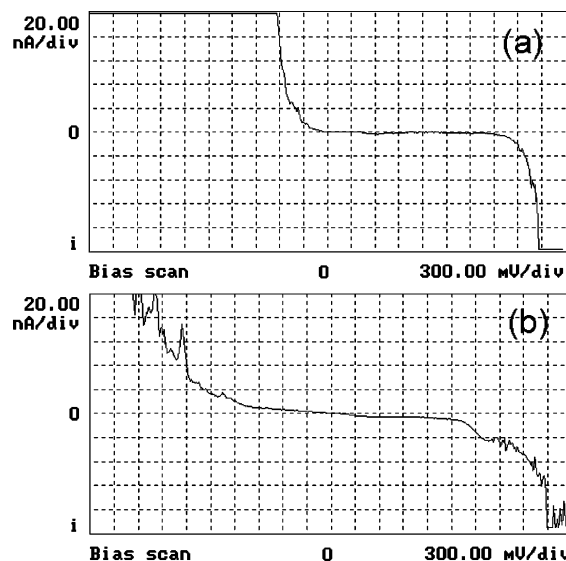


Figure 6. Scanning tunneling spectroscopy curves for fresh (a) and photoactivated (b) CdSe@CdS with a Cd/Se ratio of 4:1.

6. The current onset in the area of negative potentials, that is, when the graphite surface under the particles is negatively charged, with the tip being the positive (grounded) side of the circuit, is considerably more positive for the freshly made NPs (Figure 6), -300 mV, than for those that have been irradiated for 4 days, -900 mV. The other half of the STS curve, which corresponds to the transport of electrons in the opposite direction, is much less affected. The width of the STS curve is related to the apparent band gap of the semiconductor. The overall band-gap window in the nonilluminated state is 2.1 eV, whereas after the illumination, it becomes 2.3–2.7 eV, which corresponds to an emission wavelength of 540 nm. This leads to important conclusions about the nature of emissive and nonemissive states: (1) From Figure 2, one can see that the blue shift of the absorption band after illumination for 4 days is quite small, $\Delta\lambda \approx -10$ nm. It corresponds to an energy change of 0.065 eV and thus cannot be the reason for such a strong increase in the band-gap window in STS curves. (2) The STS band gap (Figure 6b) in the illuminated state coincides very well with the observed optical band gap determined from the UV–vis absorption spectra (Figure 2), that is, 2.3 eV, whereas the dark state underestimates it. Both of these conclusions point to the fact that in as-made NPs some of the midband-gap states are occupied, which results in the apparent reduction of the band-gap window in STS curves. These midband-gap states are most likely to be populated because of negatively charged surface defects, which indeed should affect the left, negative side of STS curve much more strongly than the right, positive side (Figure 6).

Photoactivation of CdSe@CdS@SiO₂. The enhancement of luminescence intensity was also studied on silica-coated NPs (Figure 7). We find that the activation process is faster for silica-coated NPs than for the uncoated ones. Figure 7 shows that the maximum intensity was reached in 3–4 days for the coated NPs, whereas several weeks were needed for the uncoated ones. Additionally, we observed that the blue shift is faster ($\Delta\lambda = -36$ nm after 6 days) compared to uncoated particle dispersion ($\Delta\lambda = -36$ nm after 2 weeks). This is quite surprising because previous silication of CdS NPs was observed to slow the photocorrosion processes.³⁴ As we will see later, closer examination of the phenomenon shows that these observations actually confirm that photoactivation is intrinsically related to particle photooxidation.

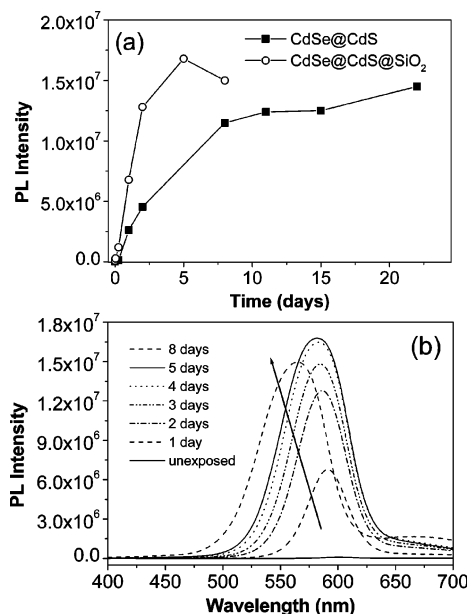


Figure 7. (a) Time evolution of the maximum PL intensity during illumination in air of CdSe@CdS and CdSe@CdS@SiO₂ nanoparticles. (b) PL spectra of CdSe@CdS@SiO₂ NPs at various illumination times.

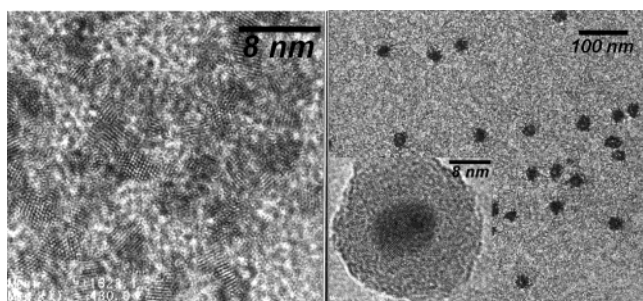


Figure 8. HRTEM micrographs of CdSe@CdS (a) and CdSe@CdS@SiO₂ (b) with a Cd/Se ratio of 4:1.

Transmission Electron Microscopy. HRTEM images obtained before and after photoactivation did not reveal any drastic change of NP morphology. It is important to note that the deposition of the CdS shells on CdSe NPs resulted in a uniform increase in their diameters. Every examined particle revealed EDAX signals both from S and Se. The continuity of the CdS shell is difficult to establish from microscopy data because of the closeness of CdS and CdSe lattice constants. Figure 8 shows micrographs of CdSe@CdS and CdSe@CdS@SiO₂ NPs. Unlike CdS, the shell made from SiO₂ is perfectly visible, and one can clearly see the virtually ideal coating without any distinguishable defects. However, the high-resolution images (inset of Figure 8b) indicate that each coated particle actually involves a core made of small aggregates of the primary CdSe@CdS NPs. It is interesting, however, that the size of such NP clusters is fairly uniform, as can be seen in the low-magnification image.

Discussion

For semiconductor NPs, the band-edge emission has to compete with nonradiative decay channels leading to surface electronic states. Strategies to enhance the photoluminescence QY aim to reduce nonradiative recombination by reducing surface defects and to confine the wave function of the electron–hole pair to the interior of the crystallite. The weak luminescence observed in the CdSe samples before light irradiation indicates that a significant number of nonradiative recombination centers

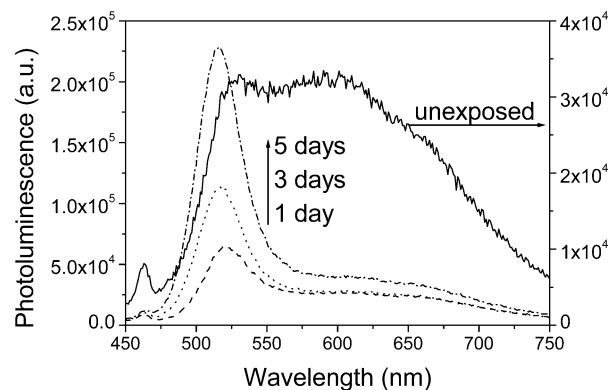


Figure 9. Emission spectra of nanocrystalline CdSe (Cd/Se 20:1) measured after different illumination times (1 day, 3 days, 5 days) in air. The intensity scale on the right is for the unexposed sample; the scale on the left is for all other samples.

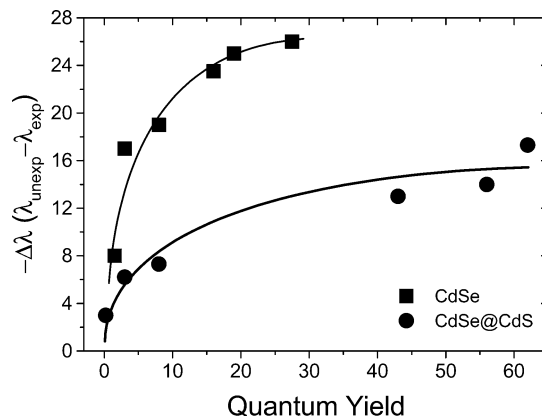


Figure 10. Shift of PL wavelength vs quantum yield during illumination of CdSe and CdSe@CdS quantum dots (Cd/Se 8:1) in air.

are present. The dramatic increase of QY, the data on surface charge (Table 2), and the STS curves (Figure 6) suggest that the photoactivation processes lead to annealing/restructuring of the surface and thereby removal of defects. Most of the time, there is no question that some restructuring does occur because photoactivation is accompanied by photocorrosion. However, the causative relationship between these two processes still needs to be explored.

Let us take CdSe nanocrystals with a Cd/Se molar ratio of 20:1 (Figure 9). For these relatively small CdSe NPs, the surface-to-volume ratio is extremely high. The luminescence for the freshly made NPs is dominated by broad, deep trap emission due to incomplete surface passivation (Figure 9, unexposed), whereas after photoactivation, the band-edge emission is strongly enhanced. Interestingly, trap emission also slightly increases during illumination, although to a much smaller extent than the band-edge emission, becoming more defined and narrow while shifting to the red. This suggests that both the number and variety of surface states dramatically decrease primarily at the expense of the defects lying close to the conduction band.

Further evidence of the close relationship between photocorrosion and photoactivation is provided by the plots in Figure 10, where the blue shift of the PL peak is plotted versus QY during illumination in the presence of oxygen. From the plots, it is evident that degradation preferentially occurs during the first stages of the illumination, with a modest increase in QY, whereas at later times, QY notably increases with a small variation in particle size. Thus, one can conclude that the increase in the luminescence intensity occurs only after a certain

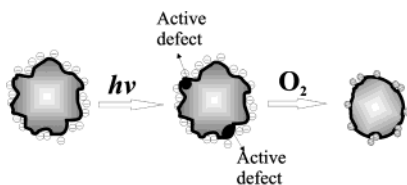
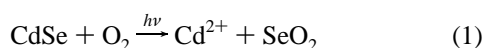


Figure 11. Suggested schematics of photoinduced luminescence enhancement. Photoinduced charge carriers are trapped in “roughness states” (active defect) on the surface. Photooxidation eliminates the surface roughness of the NP, i.e., atomic-scale imperfections. This procedure results in reduced-size NPs and yields NPs with reduced surface defects and enhanced photoluminescence.

degree of surface modification and oxidation is achieved. This threshold is greater for “naked” nanoparticles than for CdS-coated ones.

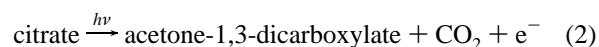
The observed differences between the emission spectra of both CdSe and CdSe@CdS core-shell NPs in air and in nitrogen indicate that the concomitant blue shift is certainly due to the aerial oxidation of CdSe nanocrystals.³⁹ X-ray photoelectron spectroscopy (XPS) results (not shown) indicate that SeO₂ is marginally present in the particles after long irradiation times, which confirms this point. The reaction that may lead to this product is the following⁴⁰



The photooxidation was also previously implicated in the increase in luminescence efficiency, related to the photoanodic dissolution of ZnS NPs proposed by Henglein.⁴⁰ Alternatively, in a control experiment, core-shell NPs were kept in the dark with continuous oxygen flow. After several days, the QY did not show any pronounced increase, which implies that light renders the annealing procedure at the surface of NPs, in which particle size remains unchanged. A similar mechanism has been suggested by Manna et al., in which laser irradiation induces a structural reorganization in CdS or ZnS shells over CdSe cores.²⁸ However, the situation is different for citrate-stabilized NPs because CdSe/TOP/TOPO nanocrystals should have a significantly lower number of surface defects because of the high synthesis temperature.

Thus, every piece of experimental data, from STS to luminescence spectra and zeta-potential measurements as well as some literature data, points to the fact that certain midband-gap states and, therefore, certain atomic structures disappear as a result of photoactivation. Combined with the observations about the ubiquitous blue shift of the optical characteristics, one can come to the conclusion that the enhancement of the luminescence is related to the removal of specific structures on the surface. Previously, it was observed that the emission of CdTe and InP nanoparticles could vary drastically depending of the smoothness of the surface.^{41,42} Consequently, the following mechanism for photoactivation in CdSe NPs is proposed. Charge carriers resulting from the adsorption of light are trapped in the surface states formed because of the uneven atomic-scale topography of NPs. The excitons activate the reactions with oxygen present in the environment, for instance, the transfer of a photoexcited electron to O₂ leading to O₂^{•−}. The remaining hole also trapped on the surface oxidizes the Se to SeO₂. This results in the gradual erosion of the unwanted topographic features on the surface and in smooth, highly luminescent NPs where the nonradiative decay of excitons no longer dominates. This proposed mechanism is schematically presented in Figure 11.

In various possible models of photoactivated luminescence, it is important to discern the cause and the consequence of the phenomenon. Jones et al. assigned the increase in quantum efficiency upon illumination to chemical changes in the particles due to the redistribution of surfactant molecules on their surfaces.³⁰ They also mention that oxygen is important, which does not really fit with surfactant reorganization. The smoothing of the surfaces of NPs will cause a number of effects, including the restructuring of the stabilizer shell, which is composed of citrate molecules in this system. However, it seems that the redistribution of the citrate adsorbed to the semiconductor NPs cannot cause such a profound change in the electronic structure as it appears here. Under some conditions, for instance, in an anaerobic environment and at high pH (Figure 5), it is possible that the reduction of citrate anions in water^{43,44}



can cause some degree of activation due to the filling of the surface electron traps. Moreover, it results in the reduction of surface charges, which is in agreement with the decrease in the zeta potential (Table 2).

Putting forward this relatively simple photoactivation mechanism (Figure 11) also raises quite a few questions related to its feasibility in different systems. For example, from Table 1 and other data (Figures 1–3, 9, and 10), we can see that photooxidation occurs to both bare CdSe and CdSe@CdS core-shell NPs. Now the question is, how can CdSe photocorrosion occur under the CdS shell? Oxygen in the scheme in Figure 11 can react only with the atoms located at the NP–water interface. Moreover, the photoenhancement of luminescence in CdS-coated CdSe can not only be observed but also is always greater than that in naked CdSe. To explain this observation, we hypothesize that (1) the CdS shell on CdS cores is incomplete and (2) it is deposited only on a previously smooth and nearly perfect CdSe lattice. Considering that CdS deposition on CdSe has epitaxial character,^{45–47} this hypothesis appears to be very feasible. Additionally, if there are grain boundaries of CdS crystallites on the surface, then oxygen can diffuse toward the CdSe core inside the CdS shell. Similar phenomena were also observed by van Sark³⁷ for the photooxidation of single CdSe@ZnS NPs.

Being armed by this hypothesis, let us see now if we can explain the experimental data for core-shell NPs. As one can expect from this model, the blue shift for naked CdSe NPs during photooxidation is much larger than that for the corresponding core-shell nanocrystals (Table 1, Figures 3 and 10). This is caused by a smaller number of surface defects due to overcoating with a higher band-gap CdS shell, which, to some extent, resists photooxidation. STS data indicate that there is indeed significant expansion of the CdSe apparent band gap, which greatly exceeds the reduction of particle size. This can occur only if parts of the CdSe surface—not CdS—are exposed to a reaction with oxygen. The relative reduction of the zeta potential (Table 2) is not as pronounced as that for naked CdSe, which shows that a smaller surface of NPs is being affected.

We note that the photocorrosion of CdS shells can also occur. Photogenerated holes can indeed oxidize both S^{2−} and Se^{2−}. However, this process does not notably affect either absorption or luminescence in these core-shell NPs. Considering atomic-scale movements at the interfaces, we must also point out that once some area of the CdSe surface becomes atomically smooth the CdS shell can spontaneously diffuse and cover it in epitaxial manner, thereby expanding the area with a protected surface.

This process can certainly be facilitated by the presence of Cd^{2+} ions in the solution. In addition, atomic diffusion at the interfaces has been observed in many instances, including CdSe and similar II–VI semiconductors at room temperature.^{48–51} Certainly, the process of shell expansion initiated by photooxidation cannot lead to complete CdS coverage and thick shells because some oxygen would then start to corrode the CdS shell. This is probably reflected by the maximum QYs (Table 1), which can be as high as 59% but still somewhat lower than those for the best examples of high-temperature synthesis⁵² when CdS is deposited on CdSe from solution. At the same time, the simple CdS coating procedure used here lends itself to the second step of CdS deposition after photocorrosion when the remaining CdSe surface is atomically smooth and ready for epitaxial deposition.

The second serious question can be raised about the high efficiency of photoactivation in CdSe@CdS NPs with thin silica shells. In ref 34, an inhibition of photodegradation was observed upon the growth of thicker shells from alkoxysilane hydrolysis and condensation in ethanol. However, for shells grown in water from sodium silicate, such as in the present case, reaction with dissolved oxygen is still possible because it has been demonstrated that silica shells grown in this way are sufficiently porous to allow chemical^{53,54} and electrochemical⁵⁵ reactions to take place on the cores. Our results (Figure 7) show that photoactivation not only takes place but also occurs at a faster rate than for noncoated NPs. This apparent controversy can be resolved by recalling the fact that the porosity of the silicate shell also results in the enhanced adsorption of oxygen from solution.⁵⁶ Oxygen trapped within the pores of the silica shell is more readily available for the photocorrosion reactions and therefore for the photoactivation process.

Conclusions

The luminescence quantum yield of both CdSe and CdSe@CdS core–shell NPs can be dramatically enhanced upon illumination in the presence of oxygen. After photoactivation, naked CdSe NPs show a QY of up to 20%, compared to 0.01–0.43% QY in the as-prepared state. In terms of emitted light intensity, this corresponds to an increase of about 2 orders of magnitude. The blue shift of the emission and absorption bands during irradiation of NPs in air points toward particle-size reduction. On the basis of a variety of qualitative and quantitative data, one can conclude that the essence of the photoactivation is elimination of topological surface defects, that is, the smoothing of the NP surface, during photocorrosion. The phenomenon of photoactivation is surprisingly robust for citrate-stabilized CdSe NPs and can also be observed after coating with CdS and SiO_2 . Moreover, porous silicate layers accelerate the activation process because of the concentration of oxygen in the shell. The QY of core–shell CdSe@CdS NPs was observed to be as high as 59.0%, which is probably the record for aqueous CdSe dispersions and approaches the QY for thiol-stabilized NPs of CdTe and TOP/TOPO-stabilized CdSe by carrying the passivating shell from wide band-gap material. Efficient photoactivation of CdSe@CdS dispersions leads to the assumptions of the incompleteness of the CdS layer on as-made colloids and atomic diffusion of the CdS layer at CdSe–water interface.

It should probably be emphasized that this described process may be considered to be a synthetic method of highly luminescent semiconductor dispersions. It is exceptionally simple and free of expensive chemicals or complicated vacuum setups. Additionally, it is also environmentally and biologically friendly because the whole synthesis is carried out in water.

On the negative side, we note that the size distribution of the particles is still wider than the best examples of organic-made CdSe dispersions. This problem can also be resolved by selecting a different citratelike stabilizer.

The uniquely high contrast between activated and nonactivated states calls for a new family of applications related to optical patterning. One of the important directions of the process optimization would be the induced and controlled acceleration of the photoactivation process.

Acknowledgment. Financial support from the Spanish Ministerio de Ciencia y Tecnología (project no. BQU2001-3799) and Xunta de Galicia (project no. PGIDIT03TMT30101PR) is gratefully acknowledged. We thank Carmen Serra (C.A.C.T.I., Vigo University) for performing the XPS measurements.

References and Notes

- (1) Colvin, V. L.; Schlamp, M. C.; Alivisatos, A. P. *Nature* **1994**, *370*, 354.
- (2) Gao, M. Y.; Richter, B.; Kirstein, S.; Mohwald, H. *J. Phys. Chem. B* **1998**, *102*, 4096.
- (3) Mattoussi, H.; Radzilowski, L. H.; Dabbousi, B. O.; Thomas, E. L.; Bawendi, M. G.; Rubner, M. F. *J. Appl. Phys.* **1998**, *83*, 7965.
- (4) Gaponik, N. P.; Talapin, D. V.; Rogach, A. L. *Phys. Chem. Chem. Phys.* **1999**, *1*, 1787.
- (5) Bruchez, M.; Moronne, M.; Gin, P.; Weiss, S.; Alivisatos, A. P. *Science* **1998**, *281*, 2013.
- (6) Chan, W. C. W.; Nie, S. *Science* **1998**, *281*, 2016.
- (7) Mitchell, G. P.; Mirkin, C. A.; Letsinger, R. L. *J. Am. Chem. Soc.* **1999**, *121*, 8122.
- (8) Weller, H. *Angew. Chem., Int. Ed. Engl.* **1993**, *32*, 41.
- (9) Alivisatos, A. P. *J. Phys. Chem.* **1996**, *100*, 13226.
- (10) Peng, X. G.; Manna, L.; Yang, W. D.; Wickham, J.; Scher, E.; Kadavanich, A.; Alivisatos, A. P. *Nature* **2000**, *404*, 59.
- (11) Woggon, U. *Optical Properties of Semiconductor Quantum Dots*; Springer: Berlin, 1997.
- (12) Murray, C. B.; Norris, D. J.; Bawendi, M. G. *J. Am. Chem. Soc.* **1993**, *115*, 8706.
- (13) Vossmeier, T.; Katsikas, L.; Giersig, M.; Popovic, I. G.; Diesner, K.; Chemseddine, A.; Eychmüller, A.; Weller, H. *J. Phys. Chem.* **1994**, *98*, 7665.
- (14) Peng, Z. A.; Peng, X. *J. Am. Chem. Soc.* **2001**, *123*, 183.
- (15) Bol, A. A.; Meijerink, A. *J. Phys. Chem. B* **2001**, *105*, 10197.
- (16) Spanhel, L.; Haase, M.; Weller, H.; Henglein, A. *J. Am. Chem. Soc.* **1987**, *109*, 5649.
- (17) Danek, M.; Jensen, K. F.; Murray, C. B.; Bawendi, M. G. *Chem. Mater.* **1996**, *8*, 173.
- (18) Hoener, C. F.; Allan, K. A.; Bard, A. J.; Campion, A.; Fox, M. A.; Mallouk, T. E.; Webber, S. E.; White, J. M. *J. Phys. Chem.* **1992**, *96*, 3812.
- (19) Hines, M. A.; Guyot-Sionnest, P. *J. Phys. Chem.* **1996**, *100*, 468.
- (20) Kortan, A. R.; Hull, R.; Opila, R. L.; Bawendi, M. G.; Steigerwald, M. L.; Carroll, P. J.; Brus, L. E. *J. Am. Chem. Soc.* **1990**, *112*, 1327.
- (21) Mews, A.; Eychmüller, A.; Giersig, M.; Schooss, D.; Weller, H. *J. Phys. Chem.* **1994**, *98*, 934.
- (22) Mews, A.; Kadavanich, A. V.; Banin, U.; Alivisatos, A. P. *Phys. Rev. B* **1996**, *53*, 13242.
- (23) Tian, Y.; Newton, T.; Kotov, N. A.; Guldi, D. M.; Fendler, J. H. *J. Phys. Chem.* **1996**, *100*, 8927.
- (24) Rogach, A. L.; Nagesha, D.; Ostrander, J. W.; Giersig, M.; Kotov, N. A. *Chem. Mater.* **2000**, *12*, 2676.
- (25) Wang, Y.; Tang, Z.; Correa-Duarte, M. A.; Liz-Marzán, L. M.; Kotov, N. A. *J. Am. Chem. Soc.* **2003**, *125*, 2830.
- (26) Patterson, G. H.; Lippincott-Schwartz, J. *Science* **2002**, *297*, 1873.
- (27) Bol, A. A.; Meijerink, A. *J. Phys. Chem. B* **2001**, *105*, 10203.
- (28) Manna, L.; Scher, E. C.; Li, L.-S.; Alivisatos, A. P. *J. Am. Chem. Soc.* **2002**, *124*, 7136.
- (29) Cordero, S. R.; Carson, P. J.; Estabrook, R. A.; Strouse, G. F.; Buratto, S. K. *J. Phys. Chem. B* **2000**, *104*, 12137.
- (30) Jones, M.; Nedeljkovic, J.; Ellingson, R. J.; Nozik, A. J.; Rumbles, G. *J. Phys. Chem. B* **2003**, *107*, 11346.
- (31) Gaponik, N.; Talapin, D. V.; Rogach, A. L.; Hoppe, K.; Shevchenko, E. V.; Kornowski, A.; Eychmüller, A.; Weller, H. *J. Phys. Chem. B* **2002**, *106*, 7177.
- (32) Harrison, M. T.; Kershaw, S. V.; Rogach, A. L.; Kornowski, A.; Eychmüller, A.; Weller, H. *Adv. Mater.* **2000**, *12*, 123.
- (33) Henglein, A. *Ber. Bunsen-Ges. Phys. Chem.* **1982**, *86*, 301.
- (34) Correa-Duarte, M. A.; Giersig, M.; Liz-Marzán, L. M. *Chem. Phys. Lett.* **1998**, *286*, 497.
- (35) Nirmal, M.; Brus, L. *Acc. Chem. Res.* **1999**, *32*, 407.

- (36) Nirmal, M.; Dabbousi, B. O.; Bawendi, M. G.; Macklin, J. J.; Trautman, J. K.; Harris, T. D.; Brus, L. E. *Nature* **1996**, *383*, 802.
- (37) van Sark, W. G. J. H. M.; Frederix, P. L. T. M.; Van den Heuvel, D. J.; Gerritsen, H. C.; Bol, A. A.; van Lingn, J. N. J.; de Mello Donegá, C.; Meijerink, A. *J. Phys. Chem. B* **2001**, *105*, 8281.
- (38) In this case, the increase in quantum efficiency caused by decreasing particle size can be ruled out, and thus charge removal from the surface is most likely to take place through a different mechanism involving other species. At high pH, SH^- groups on the surface of the NPs are converted into S^{2-} , which can bind excess Cd^{2+} ions, possibly in the form of $\text{S}^{2-}\cdots\text{Cd}^{2+}\cdots\text{OH}^-$ structures. The removal of SH^- groups and the accumulation of Cd^{2+} on the surface thus seem to destroy the sites where radiationless recombination of the charge carriers can occur.
- (39) Bowen Katari, J. E.; Colvin, V. L.; Alivisatos, A. P. *J. Phys. Chem.* **1994**, *98*, 4109.
- (40) Henglein, A. *Top. Curr. Chem.* **1988**, *143*, 113.
- (41) Adam, S.; McGinley, C.; Möller, T.; Talapin, D. V.; Borchert, H.; Haase, M.; Weller, H. *Eur. Phys. J. D* **2003**, *24*, 373.
- (42) Borchert, H.; Talapin, D. V.; Gaponik, N.; McGinley, C.; Adam, S.; Lobo, A.; Möller, T.; Weller, H. *J. Phys. Chem. B* **2003**, *107*, 9662.
- (43) Sato, T.; Kuroda, S.; Takami, A.; Yonezawa, Y.; Hada, H. *Appl. Organomet. Chem.* **1991**, *5*, 261.
- (44) Maillard, M.; Huang, P.; Brus, L. *Nano Lett.* **2003**, *3*, 1611.
- (45) Li, J. J.; Wang, Y. A.; Guo, W.; Keay, J. C.; Mishima, T. D.; Johnson, M. B.; Peng, X. *J. Am. Chem. Soc.* **2003**, *125*, 12567.
- (46) Mekis, I.; Talapin, D. V.; Kornowski, A.; Haase, M.; Weller, H. *J. Phys. Chem. B* **2003**, *107*, 7454.
- (47) Peng, X.; Schlamp, M. C.; Kadavanich, A. V.; Alivisatos, A. P. *J. Am. Chem. Soc.* **1997**, *119*, 7019.
- (48) Schallenberg, T.; Schumacher, C.; Brunner, K.; Molenkamp, L. W. *Phys. Status Solidi B* **2004**, *241*, 564.
- (49) Kim, M.; Furdyna, J. K.; Dobrowolska, M.; Lee, S.; Cheon, M.; Luo, H. *Appl. Phys. Lett.* **2003**, *83*, 1728.
- (50) Yang, Y.; Shen, D. Z.; Zhang, J. Y.; Fan, X. W.; Zhen, Z. H.; Zhao, X. W.; Zhao, D. X.; Liu, Y. N. *J. Cryst. Growth* **2001**, *225*, 431.
- (51) Nakada, T.; Kunioka, A. *Appl. Phys. Lett.* **1999**, *74*, 2444.
- (52) Wang, X.; Qu, L.; Zhang, J.; Peng, X.; Xiao, M. *Nano Lett.* **2003**, *3*, 1103.
- (53) Ung, T.; Liz-Marzán, L. M.; Mulvaney, P. *Langmuir* **1998**, *14*, 6430.
- (54) Liz-Marzán, L. M.; Mulvaney, P. *Recent Res. Dev. Phys. Chem.* **1998**, *2*, 1.
- (55) Ung, T.; Liz-Marzán, L. M.; Mulvaney, P. *J. Phys. Chem. B* **1999**, *103*, 6770.
- (56) Zhang, P.; Guo, J.; Wang, Y.; Pang, W. *Mater. Lett.* **2002**, *53*, 400.